Journal of Asian Ceramic Societies 4 (2016) 81–84

Journal of Asian Ceramic Societies

journal homepage: www.elsevier.com/locate/jascer

Electrical and optical properties of CZTS thin films prepared by SILAR method

J. Henry [a], K. Mohanraj [a,*], G. Sivakumar [b]

[a] Department of Physics, Manonmaniam Sundaranar University, Tirunelveli 627 012, Tamil Nadu, India
[b] Centralised Instrumentation and Service Laboratory, Department of Physics, Annamalai University, Annamalai Nagar 608 002, Tamil Nadu, India

ARTICLE INFO

Article history:
Received 22 September 2015
Received in revised form
19 November 2015
Accepted 3 December 2015
Available online 30 December 2015

Keywords:
Thin films
Absorption
Sol–gel
Chalcogenides
Semiconductors

ABSTRACT

In the present work, Cu_2ZnSnS_4 (CZTS) thin film was deposited onto the glass substrate by simple and economic SILAR method and its structural, morphological, optical and electrical properties were analyzed. X-ray diffraction (XRD) analysis confirms the formation of CZTS with kesterite structure and the average crystallite size is found to be 142 nm. Scanning electron microscope (SEM) image shows that the film has homogeneous, agglomerated surface without any cracks. The prepared CZTS film shows good optical absorption (10^4 cm^{-1}) in the visible region and the optical band gap energy is found to be quite close to the optimum value of about 1.54 eV for solar cell application. The refractive index of the prepared film is found to be 2.85. The electrical resistivity of the film is found to be $\sim 10^{-2}$ Ω cm at room temperature.

1. Introduction

Optical property of thin films found a large number of disparate applications in science and technology coatings [1]. Cu_2ZnSnS_4 (CZTS) film has gained much interest in recent years, due to the fact that its optical property is optimum (1.4–1.5 eV) for photovoltaic application [2]. CZTS is a p-type semiconductor which has an optimum band gap, and large absorption coefficient (>10^4 cm^{-1}) makes it an alternate potential candidate for thin film solar cells [3].

Recently, Noriko Moritake et al. have reported the fabrication of CZTS thin film solar cells by the sol–gel method by the sulfurizing of precursors. The structure of the solar cells was Al/ZnO:Al/CdS/CZTS/Mo/Soda Lime Glass substrate and the Power Conversion Efficiency (PCE) of the cell was 1.61% [4]. Sudip K. Saha et al. prepared CZTS-fullerene hybrid p–n junction solar cells by hot injection method and have reported 0.9% PCE [5]. Jin Woo Cho et al. reported the PCE of 3.02% for spin coated CZTS thin films [6]. Subramaniam et al. have reported 1.34% PCE for CZTS film deposited by chemical bath deposition method [2]. Suryawansi et al. prepared CZTS by SILAR method and obtained PCE of about 3.81% [7]. The reported experimental studies have shown that the PCE of CZTS film varies considerably by preparation methods such as RF sputtering [8], electron beam evaporation [9], thermal evaporation [10], spray pyrolysis [11], spin coating [12], pulsed laser deposition [13], electrodeposition process [14] and SILAR method [15]. The main drawback of these methods is that they require sulfurization for CZTS film formation, in which either N_2 or H_2S atmosphere is required for annealing [7]. To overcome the drawback, Successive Ionic Layer Adsorption and Reaction (SILAR) method is the preferable one which is very simple, cheap and suitable for making uniform and large area thin films. This SILAR method is relatively a new and less investigated method. In addition, this method is also suitable for metal sulfide, selenides, tellurides and oxides [16–18]. In this method, thin films are obtained by immersing the substrate directly into anionic and cationic precursors and rinsing between every immersion with distilled water. On the other hand, literature survey shows that there are only a few reports [7,15–17] available on the synthesis of CZTS thin film using SILAR route. The authors have studied its structural, optical and PEC studies of the SILAR deposited CZTS thin films. Hence, the objective of the work is to deposit CZTS thin film on transparent glass substrate and to study its structural, optical and electrical properties.

2. Experimental

In this study CZTS thin film was deposited on glass substrate using SILAR method at room temperature. A.R. grade of $CuSO_4$,

* Corresponding author. Tel.: +91 9788083079; fax: +91 462 2334363/2322973.
E-mail addresses: kmohanraj.msu@gmail.com, mohanraj@msuniv.ac.in (K. Mohanraj).

Peer review under responsibility of The Ceramic Society of Japan and the Korean Ceramic Society.

http://dx.doi.org/10.1016/j.jascer.2015.12.003

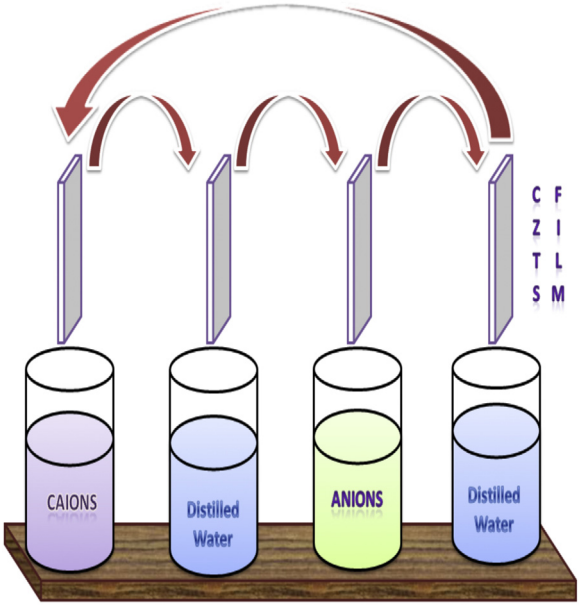

Fig. 1. Schematic representation of CZTS thin film deposited by SILAR method.

$ZnSO_4$, $SnCl_2$ and Na_2S precursor were used without any modification. Substrate cleaning plays an important role in the preparation of thin films and the cleaning process was adopted according to the earlier report [19].

The experimental process consists of four beakers: the first beaker contains mixed cationic precursor solution (40 ml) of 0.1 M $CuSO_4$, 0.05 M $ZnSO_4$ and 0.05 M $SnCl_2$, the second beaker has sufficient amount of distilled water to remove loosely adsorbed cations from the substrate, the third beaker consists of 0.2 M Na_2S anionic precursor solution and the fourth beaker contains double distilled water to remove the powdery deposit or precipitate on the substrate. In this method, the growth kinetics of a thin film deposition process involves ion-by-ion deposition at nucleation sites on the immersed surfaces.

In typical deposition, substrates were immersed separately in cation and anion precursor solution with simultaneous rinsing by using distilled water between every immersion to avoid any precipitation. First the ultrasonically cleaned substrate was immersed vertically into the cationic precursor solution for 30 s in which cations ions are adsorbed on the glass substrate. Consequently the substrate rinsed with distilled water for 10 s to remove the loosely bonded ions was again immersed into the anionic precursor solution for 30 s where the anions react with the pre-adsorbed cations to form CZTS layer on a glass substrate and finally rinsed with distilled water for 10 s to remove the unreacted cation ions, anions and loosely bonded powdery CZTS particles. The above four steps (Fig. 1) form one SILAR cycle. Similarly, 70 SILAR cycles were made to deposit CZTS thin film. The deposited films were annealed at 250 °C for 2 h in air atmosphere.

The film thickness was determined by using the standard procedure [20] and it is found to be 177 nm. The structural characteristics of films were characterized by using Cu Kα (PANalytical X'Pert Pro Powder diffractometer) monochromatic radiation source (λ = 1.5406 Å) in the range of $2\theta = 10°–80°$. The surface morphology of the film was recorded using scanning electron microscope (JEOL SEM model JEM-5610 LV). Optical absorption spectrum was recorded using JASCO UVIDEC – 650 UV–Vis spectrophotometer and electrical property of the film was measured by using AUT85670 setup.

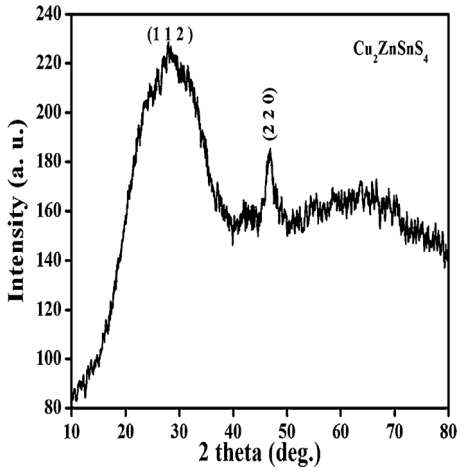

Fig. 2. XRD pattern of CZTS thin film.

3. Results and discussion

Fig. 2 shows the XRD pattern of CZTS thin film that indicates characteristic peak (2 2 0) and (1 1 2) corresponding to kesterite structure [JCPDS card no. 26-0575]. Similarly R. Lydia and P. Sreedhara Reddy prepared CZTS nanoparticles with a major peak along (2 2 0) by co-precipitation [21]. The wide peak from $2\theta = 10–30°$ may be attributed to the glass substrate.

The crystallite size was estimated by using Scherrer's formula [15]

$$D = \frac{0.9\lambda}{\beta \cos\theta} \quad (1)$$

where β is full width at half maximum (FWHM), λ is the wavelength of X-ray source, θ is the Bragg's angle. The prepared CZTS film is polycrystalline in nature, and hence large number of grains with various relative positions and orientations cause variations in the phase difference between the wave scattered by one grain and the others. The total intensity scattered by all grains is the sum of individual intensities scattered by each grain [22]. On the other hand, the stresses are one of the most important unfavorable factors affecting the structural properties that can result from geometric mismatch at boundaries between crystalline lattices of films and substrate [23]. These stresses can cause microstrains (e) in the films.

The microstrain can be calculated from the following relation [24]

$$\varepsilon = \frac{\beta \cos\theta}{4} \quad (2)$$

A dislocation is an imperfection in a crystal associated with the misregistry of the lattice in one part of the crystal with that in another part. Unlike vacancies and interstitial atoms, dislocations are not equilibrium imperfections [25]. The regular patterns are interrupted by dislocations or crystallographic defects [26].

The dislocation density (δ) was evaluated by the formula [21]

$$\delta = \frac{1}{D^2} \quad (3)$$

The stacking fault probability α is the fraction of layers undergoing stacking sequence faults in a given crystal and hence one fault is expected to be found in $1/\alpha$ layers. The presence of stacking faults gives rise to a shift in the peak positions of different reflections with respect to ideal positions of a fault-free well-annealed sample [27]. The stacking fault probabilities were calculated from the shift of the X-ray line of the film with reference (JCPDS database No: 26-0575),

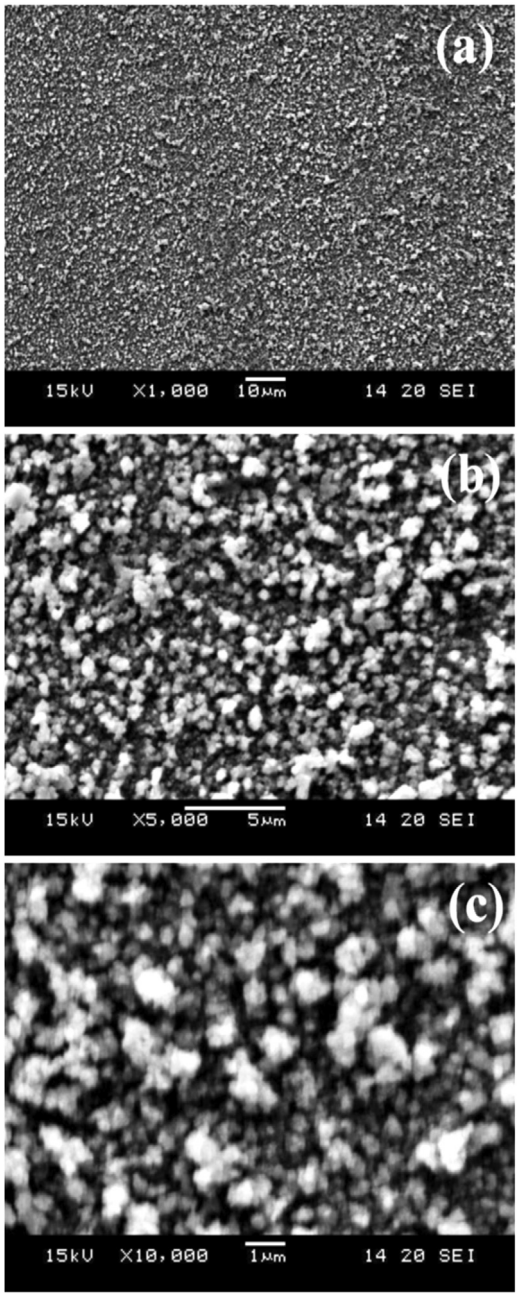

Fig. 3. SEM images of CZTS thin film.

using the relation between the stacking fault probability α and the peak shift $\Delta(2\theta)$ [10].

$$\alpha = \left[\frac{2\pi^2}{45\sqrt{3}\tan\theta}\right]\Delta(2\theta) \quad (4)$$

The crystallite size, dislocation density, microstrain and stacking fault probability are found to be 142 nm, 5×10^4 lines/m^2, 2.4×10^{-3} and 0.00214, respectively.

Fig. 3(a and b) shows the SEM image of the deposited CZTS thin film that indicates the deposited CZTS thin films are uniform, without cracks or holes and well covered to the glass substrate (Fig. 3a). Large agglomerated grains are observed (Fig. 3c), which is beneficial in photovoltaic applications, as the recombination of the photo-generated electron will be reduced [15].

Fig. 4 shows the UV–visible spectrum of CZTS thin film. It is evident from the spectrum that the CZTS thin film has high absorbance

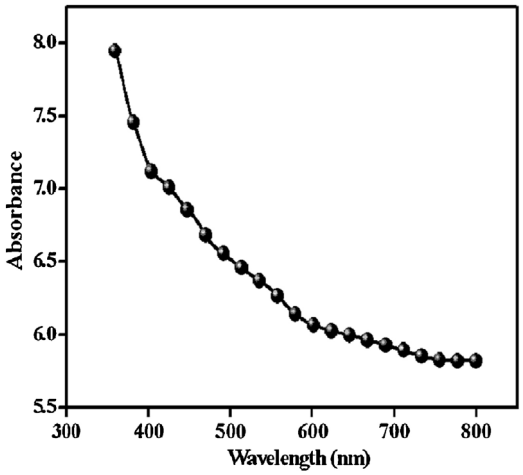

Fig. 4. UV–Vis spectrum of CZTS thin film.

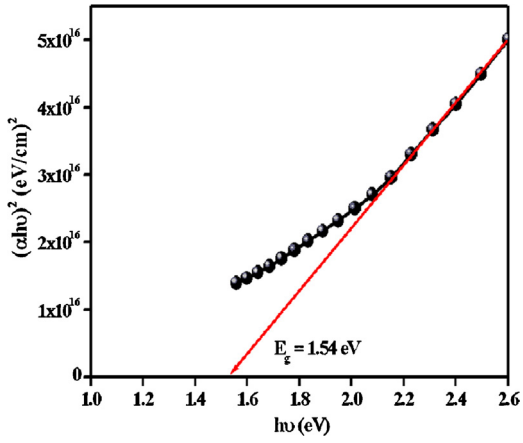

Fig. 5. E_g plot of CZTS thin film.

of light in visible region, indicating it as an absorbing material. The absorption coefficient is found to be larger than 10^4 cm^{-1} in the visible region, and is consistent with the earlier report [15].

The study of a material by means of optical absorption provides a simple method for explaining some features concerning the band structure of the material. Optical band gap energy is calculated using Bardeen equation as described in the earlier report [19]. The optical band gap energy of direct transitions was evaluated from the plot (Fig. 5) and that is found to be 1.54 eV. The result is in good agreement with the earlier report [28]. The band gap of the film is close to the optimum band gap required for the solar cells, indicating promising material or alternate candidate for thin film solar cell applications.

The refractive index (n) and dielectric constant (ε) of semiconducting materials are very important in determining the optical and electrical properties of the film which is essential for designing heterostructure lasers in optoelectronic devices as well as in solar cell applications. The refractive index is directly related to the fundamental energy band gap (E_g) by the Moss relation [29] equation (5)

$$E_g n^4 = k \quad (5)$$

where k is a constant with a value of 108 eV. A different relation between the refractive index and band gap energy is presented by

Table 1
Refractive index (n), optical static dielectric constant (ε_0) and optical high frequency dielectric constant (ε_∞) values of CZTS thin film.

E_g (eV)	ε_0	Equation	n	ε_∞
1.58	13.653	Moss relation	2.875	8.265
		Herve &Vandamme relation	2.907	8.4506

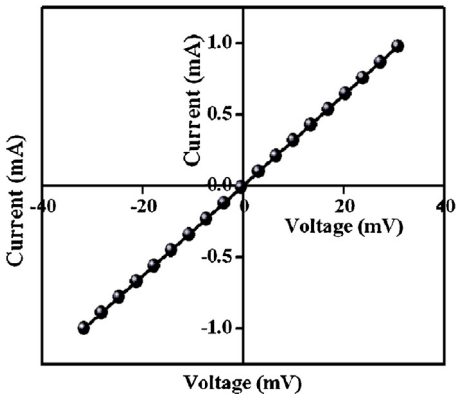

Fig. 6. *I–V* characteristics of CZTS thin film.

Herve and Vandamme. The Herve and Vandamme [24] relation is given by the following equation (6)

$$n = \sqrt{1 + \left(\frac{A}{E_g + B}\right)^2} \tag{6}$$

where A and B are numerical constants with values of 13.6 and 3.4 eV, respectively and the result is shown in Table 1. The dielectric behavior of solids is important for several electron-device properties. Both static and high frequency dielectric constants were evaluated for all the films. The high frequency dielectric constant (ε_∞) was calculated from the following relation equation (7) [29]

$$\varepsilon_\infty = n^2 \tag{7}$$

where n is refractive index. The static dielectric constant (ε_0) [24] of the films was calculated using a relation expressing the energy band gap dependence of ε_0 for semiconductors compounds in the following form equation (8)

$$\varepsilon_\infty = 18.52 - 3.08E_g. \tag{8}$$

The calculated n, ε_∞ and ε_0 values of the CZTS films are presented in Table 1.

Fig. 6 shows the *I–V* characteristics of CZTS thin film. Ohmic behavior and linear behavior were observed in the *I–V* curve of CZTS thin films. The sheet resistance and resistivity can be calculated by using the formula equations (9) and (10) [30]

$$R_{\text{Sheet}} = 4.53\left(\frac{V}{I}\right) \tag{9}$$

$$\rho = R_{\text{Sheet}}t \tag{10}$$

where R_{Sheet} is the sheet resistance, V is voltage, I is current and V/I is taken from the slope of the straight line, t is the film thickness, ρ is the resistivity. The calculated R_{Sheet} and ρ are found to be 143 Ω and 2.53×10^{-3} Ω cm (0.253×10^{-2} Ω cm), respectively. The result is in good agreement with the earlier report of CZTS thin film prepared by chemical bath deposition method [31].

4. Conclusion

In summary, the CZTS thin film was deposited by SILAR method and was characterized by XRD, SEM, UV–Vis and *I–V* characterization. The XRD pattern confirms the formation of kesterite structure CZTS thin films and agrees with the other deposited methods. The SEM image shows uniform and homogeneous surface of the compound. The band gap and the refractive index are found to be around 1.54 eV and 2.85, respectively. The electrical resistivity value of the film is found to be $\sim 10^{-2}$ Ω cm at room temperature. Further work is being progressed for the fabrication of p–n solar cells for improving the cell efficiencies.

Acknowledgements

The authors are thankful to the UGC-BSR, New Delhi for providing fellowship and DST-FIST and UGC-SAP, New Delhi for providing the financial support to the Department of Physics, Manonmaniam Sundaranar University and the authors are thankful to the Prof. and Head, Department of Physics, Annamalai University for recording SEM images. The author J. Henry acknowledges University Grants Commission (UGC), New Delhi for providing financial support through Basic Scientific Research (BSR) fellowship.

References

[1] E. Valkonen, C.-G. Ribbing and J.-E. Sundgren, Proc. SPIE, 652, 235–242 (1986).
[2] E.P. Subramaniam, G. Rajesh, N. Muthukumarasamy, M. Thambidurai, V. Asokan and D. Velauthapillai, Indian J. Pure Appl. Phys., 52, 620–624 (2014).
[3] A.V. Kumar, N.-K. Park and E.-T. Kim, Phys. Status Solidi A, 211, 1857–1859 (2014).
[4] N. Moritake, Y. Fukui, M. Oonuki, K. Tanaka and H. Uchiki, Phys. Status Solidi C, 6, 1233–1236 (2009).
[5] S.K. Saha, A. Guchhait and A.J. Pal, Phys. Chem. Chem. Phys., 14, 8090–8096 (2014).
[6] J.W. Cho, A. Ismail, S.J. Park, W. Kim, S. Yoon and B.K. Min, Appl. Mater. Interfaces, 5, 4162–4165 (2013).
[7] M.P. Suryawanshi, S.W. Shin, U.V. Ghorpade, K.V. Gurav, C.W. Hong, G.L. Agawane, S.A. Vanalakar, J.H. Moon, J.H. Yun, P.S. Patil, J.H. Kimand and A.V. Moholkar, Electrochim. Acta, 150, 136–145 (2014).
[8] J.-S. Seol, S.-Y. Lee, J.-C. Lee, H.-D. Nam and K.-H. Kim, Solar Energy Mater. Solar Cells, 75, 155–162 (2003).
[9] H. Katagiri, N. Sasaguchi, S. Hando, S. Hoshino, J. Ohashi and T. Yokota, Solar Energy Mater. Solar Cells, 49, 407–414 (1997).
[10] R. Touati, M.B. Rabeh and M. Kanzari, Energy Procedia, 44, 44–51 (2014).
[11] M.E. Rodriguez, D. Sylla, Y. Sanchez, S. Lopez-Marino, X. Fontané, J. Lopez-García, M. Placidi, A. Perez-Rodríguez, O. Vigil-Galań and E. Saucedo, J. Phys. D: Appl. Phys., 47, 245101 (2014).
[12] J. Wang, P. Zhang, X. Song and L. Gao, RSC Adv., 4, 21318–21324 (2014).
[13] K. Moriya, K. Tanaka and H. Uchiki, Jpn. J. Appl. Phys., 47, 602–604 (2008).
[14] B. Ananthoju, A. Kushwaha, F.J. Sonia and M. Aslam, AIP Conf. Proc., 1512, 706–707 (2013).
[15] N.M. Shinde, D.P. Dubal, D.S. Dhawale, C.D. Lokhande, J.H. Kim and J.H. Moon, Mater. Res. Bull., 47, 302–307 (2012).
[16] S.S. Mali, B.M. Patil, C.A. Betty, P.N. Bhoslae, Y.W. Oh, S.R. Jadkar, R.S. Devan, Y.-R. Maand and P.S. Patil, Electrochim. Acta, 66, 216–221 (2012).
[17] S.S. Mali, P.S. Shinde, C.A. Betty, P.N. Bhosale, Y.W. Oh and P.S. Patil, J. Phys. Chem. Solids, 73, 735–740 (2012).
[18] M.A. Yildirim, A. Ates and A. Astam, Physica E, 41, 1365–1372 (2009).
[19] N. Sabli, Z.A. Talib, W.M.M. Yunus, Z. Zainal, H.S. Hilal and M. Fujii, Mater. Sci. Forum, 756, 273–280 (2013).
[20] E. Riverous, E. Romero and G. Goridllo, Brazil. J. Phys., 36, 1042–1045 (2006).
[21] R. Lydia and P.S. Reddy, J. Nano-Electron. Phys., 5, 03017 (2013).
[22] B.G. Jeyaprakash, K. Kesavan, R.A. Kumar, S. Mohan and A. Amalarani, Bull. Mater. Sci., 34, 601–605 (2011).
[23] G. Turgut, E.F. Keskenler, S. Aydin, S. Dogan, S. Duman, S. Özçelik, B. Gürbulak and B. Esen, Phys. Status Solidi A, 211, 580–586 (2014).
[24] Rahul, S.R. Vishwakarma, R.N. Tripathi and A.K. Verma, Afr. Rev. Phys., 6, 103–110 (2011).
[25] P.K.R. Kalita, B.K. Sarma and H.L. Das, Bull. Mater. Sci., 23, 313–317 (2000).
[26] G.S. Thool, A.K. Singh, R.S. Singh, A. Gupta and M.A.B.H. Susan, J. Saudi Chem. Soc., 18, 712–721 (2014).
[27] T. Mahalingam, V.S. John and L.S. Hsu, J. New Mater. Electrochem. Syst., 10, 9–14 (2007).
[28] S.K. Swami, A. Kumar and V. Dutta, Energy Procedia, 33, 198–202 (2013).
[29] M.A. Yildirim, Optics Commun., 285, 1215–1220 (2012).
[30] P. Mwathe, R. Musembi, M. Munji, V. Odari, L. Munguti, A. Ntilakigwa, J. Nguu and B. Muthoka, Coatings, 4, 747–755 (2004).
[31] R. Digraskar, S. Dhanayat, K. Gattu, S. Mahajan, D. Upadhye, A. Ghuleand and R. Sharma, AIP Conf. Proc., 1512, 236–237 (2013).